Available online at www.sciencedirect.com
SCIENCE DIRECT
Bioorganic & Medicinal Chemistry Letters 16 (2006) 3434–3439
Bioorganic & Medicinal Chemistry Letters

Design and synthesis of selective keto-1,2,4-oxadiazole-based tryptase inhibitors

James T. Palmer,* Robert M. Rydzewski, Rohan V. Mendonca, David Sperandio, Jeffrey R. Spencer, Bernard L. Hirschbein, Julia Lohman, Jeri Beltman, Margaret Nguyen and Liang Liu

Celera Genomics, 180 Kimball Way, South San Francisco, CA 94080, USA

Received 2 March 2006; revised 31 March 2006; accepted 3 April 2006
Available online 27 April 2006

Abstract—Using a scaleable, directed library approach based on orthogonally protected advanced intermediates, we have prepared a series of potent keto-1,2,4-oxadiazoles designed to explore the P_2 binding pocket of human mast cell tryptase, while building in a high degree of selectivity over human trypsin and other serine proteases.

Mast cells are involved in allergic disease by virtue of pro-inflammatory mediators stored inside the secretory granules. Upon degranulation, mucosal and respiratory mast cell subpopulations release numerous effectors including the tetrameric serine protease tryptase. With trypsin-like specificity, tryptase processes substrates with immediate and long-term effects with all of the physiological responses associated with asthma. For example, tryptase activates kininogens, leading to the potent bronchoconstrictor bradykinin, and it is capable of amplifying its own signal through stimulating mast cells to further degranulate. Tryptase also processes vasoactive intestinal peptide, or down-regulating this bronchodilatory agent, and it behaves as a potent mitogen toward smooth muscle cells, endothelial cells, and fibroblasts. This effect on smooth muscle cells is of primary concern for long-term sufferers of acute asthma.[1–14] Crystallization of tryptase in 1998 by Pereira and colleagues revealed a homotetrameric structure that was amenable to structure-guided design.[15] Previously, we have described the preparation of α-ketoheterocycles elaborated with prime-side (P′) binding moieties to afford potent and selective tryptase inhibitors.[16] The best-characterized example in this series (**1**, Fig. 1) showed potency of 5.4 nM for tryptase. Our goal in this program required that we improve selectivity over trypsin and other enzymes, and to improve drug-like properties within this series. We also sought to develop a robust synthetic strategy that would allow rapid analogue preparation and large-scale synthesis of these inhibitors to support in vivo studies (See Table 1).

Our improved synthesis of [1,2,4]oxadiazole-containing tryptase inhibitors took advantage of orthogonal protecting groups as illustrated in Scheme 1. Commercially available *N*-α-benzyloxycarbonyl-*N*-ε-*tert*-butyloxycarbonyl-L-lysine **2** was converted to its *N*-α-allyloxycarbonyl derivative **4** via the Weinreb-amide **3**. Reduction to the aldehyde **5** followed by treatment with acetone cyanohydrin afforded the diastereomeric cyanohydrins **6a**,**b**. Subsequent protection as the diastereomeric TBS ethers **7a**,**b** and then conversion to the *N*-hydroxy-amidines **8a**,**b** in the presence of 50% aqueous hydroxylamine in ethanol at 50 °C provided the needed material for analogue preparation, without the need for intermediate chromatography.

Taking advantage of our distal pocket binding knowledge on the prime side of the core, we then prepared further advanced intermediates suitable for analogue exploration. The use of the 3,4-dichlorophenethyloxyphenyl group (Scheme 2) gave us not only a modest increase in potency over the lead structure **1**, but also provided us with a more facile, higher-yielding synthesis that again avoided chromatography. Mitsunobu-based coupling between 3,4-dichlorophenylethanol **9** and

Keywords: Tryptase; Serine protease; Inhibitor; Heterocycle; Keto-heterocycle; Selective; Scaleable process; Pharmacokinetics.
* Corresponding author. Tel.: +1 650 624 1341; e-mail: jpalmer@rigel.com

0960-894X/$ - see front matter © 2006 Elsevier Ltd. All rights reserved.
doi:10.1016/j.bmcl.2006.04.013

Table 1. Enzyme inhibition and pharmacokinetics data for **1**

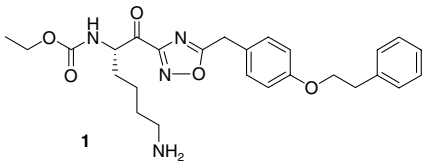

Potency (μM)	
Human B tryptase	0.0054
Selectivty (μM)	
Trypsin	0.190
Thrombin	64
Plasmin	0.43
Kallikrein	43
APC	>150
Chymotrypsin	>150
Elastase	>150
Chymase	>150
Urokinase	>150
Granzyme K	>150

methyl 4-hydroxyphenylacetate **10**, followed by saponification of the ester, extraction of neutral by-products, acidification, and filtration, permitted the product **11** to be isolated in near quantitative yield. **11** was converted to its *N*-hydroxysuccinimidoyl ester **12**, which was then coupled with **8a**,**b** under neutral conditions to give the intermediate esters **13a**,**b** and then cyclized via heating in toluene, utilizing a Dean–Stark type apparatus. The diastereomeric 1,2,4-oxadiazoles, **14a**,**b**, were then N-α-deprotected via Pd-catalyzed reductive cleavage using tributyl stannane to give **15a**,**b**, which were thus set up for the final stages of the synthesis. Although the diastereomeric nature of the intermediates (via the silyloxy group) complicated intermediate analysis, we were fortunate in discovering that one of the diastereomers of **14a**,**b** could in fact be isolated by crystallization, although at this point we did not care which one. Subsequently, the silyl group was to be removed and the secondary alcohol oxidized, thus removing the chiral center. For ease of preparation in subsequent steps, we used the crystalline material (stereochemistry unassigned) and at a later stage repeated the sequence with a mixture of **14a**,**b** and obtained similar results.

With the α-amino group now available for derivatization, we prepared a library of compounds to explore the P_2 residue of tryptase (Scheme 3). Through coupling with the appropriate acylating agent (acid chloride, aminocarbonyl chloride, isocyanate, etc.) in the presence of appropriate bases, **15a**,**b** derivatives of type **16a**,**b** were made. Deprotection of the silyl group with tetrabutylammonium fluoride gave alcohols **17a**,**b**, which were then oxidized using either Dess–Martin periodinane or through a Swern procedure to give the Boc protected, penultimate intermediate **18**. Finally, HCl-mediated deprotection of the N-ε group yielded inhibitors **19**–**44**.

Compounds **19**–**44** were assayed against tryptase and trypsin according to conditions outlined in Ref. 17. Table 2 shows the results as organized by P_2 binding moiety, represented by R^2, as attached through linker L.

While good potency was inherent in this series, thanks to the distal pocket binding moiety on the prime side, the goal of achieving several 100-fold selectivity over human trypsin required an extensive analysis of different binding elements elsewhere in the active site. In this series, we explored the effects of aliphatic and aromatic amides, carbamates, and ureas as linkers between the lysine α-amine group and the P_2-targeting group. Simple aliphatic amides (compounds **19**–**25**) showed the lowest selectivity, with only the sterically hindered (and possibly anomalous, within this series) pivalamide **36** displaying the targeted selectivity. Carbamates, both simple and extended (**26**, **27**, **30**, and **32**) showed modest (80- to 130-fold) selectivity, suggesting that the atom next to the linker carbonyl should bear minimal substituents. The ureas began to show an improvement in selectivity (**29**, **31**, and **33**–**35**) but we still felt that the intrinsic potency against trypsin was too high. When we introduced an

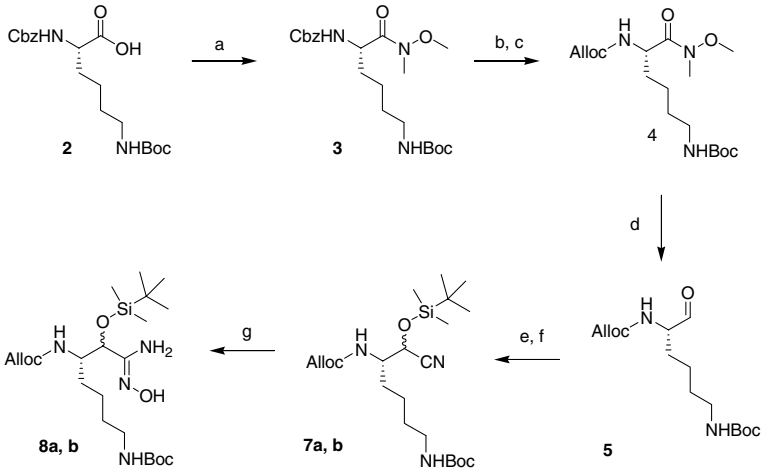

Scheme 1. Reagents and conditions: (a) *N*,*O*-Dimethylhydroxylamine, DCC, Et_3N, CH_2Cl_2, rt; (b) H_2/10% Pd, EtOH; (c) Alloc-Cl, Et_3N, THF, rt; (d) $LiAlH_4$, THF, 0 °C; (e) acetone cyanohydrin, NEt_3, CH_2Cl_2, rt; (f) TBSCl, imidazole, DMAP, CH_2Cl_2, rt; (g) NH_2OH 50 wt% in H_2O, EtOH, 50 °C.

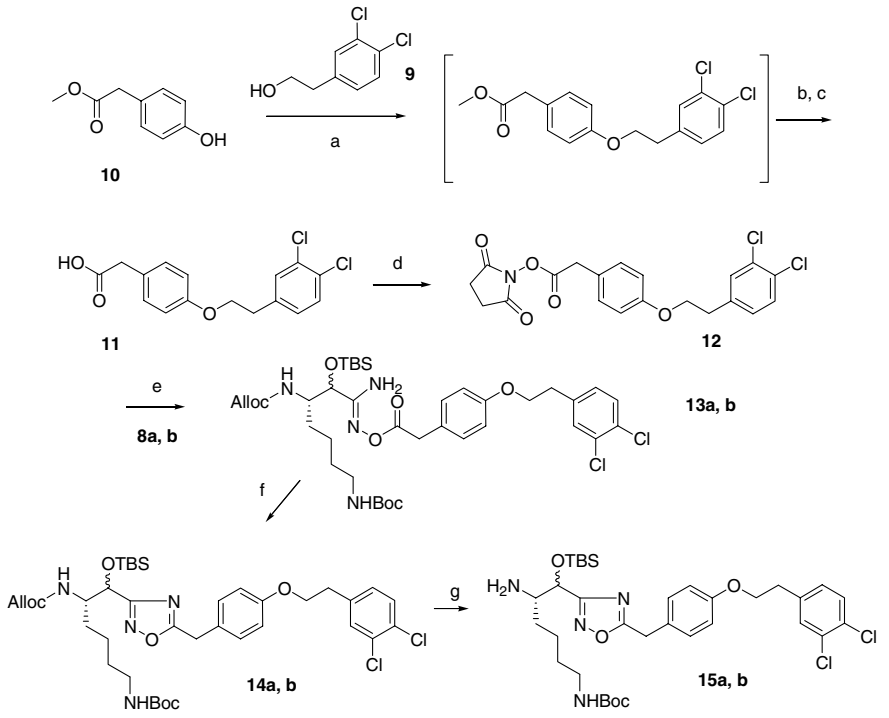

Scheme 2. Reagents and conditions: (a) PPh_3, DIAD, $CHCl_3$; (b) NaOH, THF/H_2O; (c) Et_2O extraction, followed by acidification to pH 3; (d) *N*-hydroxysuccinimide, DCC, THF, 70 °C; (e) THF, rt; (f) toluene, reflux, Dean–Stark trap; (g) $Pd(PPh_3)_4$, $BuSn_3H$, THF, rt.

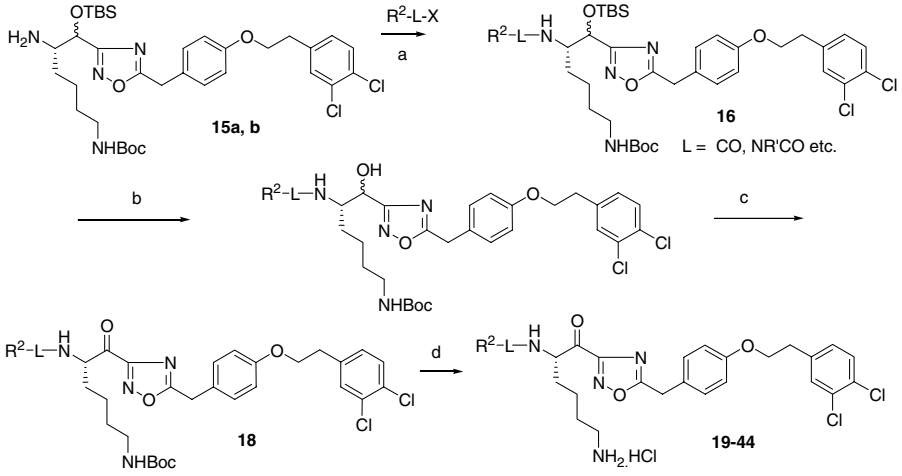

Scheme 3. Reagents and conditions: (a) Et_3N, THF etc.; (b) Bu_4NF, THF; (c) Dess–Martin periodinane, CH_2Cl_2, rt, or DMSO, $(COCl)_2$, Et_3N, CH_2Cl_2, −78 °C; (d) 4.0 M HCl/dioxane, rt.

aromatic amide at R_2, we achieved the desired increase in selectivity but not at the cost of potency, as exemplified by compounds **38**–**44**. In one case the heteroaromatic example **39** showed a modest increase in trypsin potency, so fine tuning of this substituent was clearly called for. Ultimately, the *p*-fluorobenzamide **44** displayed both the highest potency (2.5 nM) and selectivity (440-fold) over trypsin that we had yet seen in this program. The 3,4-difluorobenzamide **43** was equally selective, and we profiled this compound further against an extended panel of serine proteases. This derivative showed greater than 100-fold selectivity against over a dozen serine proteases in both trypsin and chymotrypsin-like sub-families. Table 3 indicates the results obtained.

An additional goal of this program was to improve pharmacokinetic parameters, for instance increasing terminal half-life and lowering clearance of these compounds when dosed in vivo, so that they could be used in animal models of disease. We made the initial choice of the 3,4-dichlorophenethyl group in the distal pocket to block oxidative pathways wherein unsubstituted phenyl groups might be susceptible to oxidation and rapid clearance. The same logic was applied in the use of fluorobenzamides at the P_2 position; to this

Table 2. Enzyme inhibition data for compounds **19**–**50**

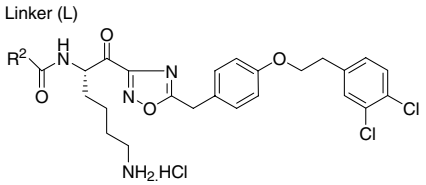

Compound	R^2	L type	Tryptase	Trypsin	Selectivity
19		Aliphatic amide	0.0046	0.044	10
20		Aliphatic amide	0.0068	0.12	18
21	*n*-Pentyl	Aliphatic amide	0.0098	0.18	18
22		Aliphatic amide	0.0065	0.3	46
23		Aliphatic amide	0.022	1.1	50
24		Aliphatic amide	0.0037	0.19	51
25	CF_3	Aliphatic amide	0.0029	0.22	76
26		Carbamate	0.0047	0.38	81
27		Carbamate	0.005	0.415	83
28		(Hetero)aromatic amide	0.046	3.9	85
29		Urea	0.0096	0.85	89
30	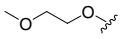	Carbamate	0.005	0.5	100
31		Urea	0.032	3.8	119
32		Carbamate	0.017	2.2	129
33		Urea	0.018	2.4	133
34		Urea	0.0092	1.4	152
35		Urea	0.0057	0.87	153
36	*t*-Bu	Aliphatic amide	0.00375	0.625	167
37	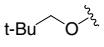	Carbamate	0.011	1.9	173
38		Aromatic amide	0.0062	1.1	177
39		(Hetero)aromatic amide	0.0023	0.48	209
40	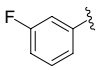	Aromatic amide	0.0058	1.7	293
41	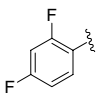	Aromatic amide	0.00325	1.15	354
42	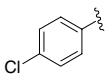	Aromatic amide	0.00655	2.55	389

(*continued on next page*)

Table 2 (*continued*)

Compound	R^2	L type	Tryptase	Trypsin	Selectivity
43		Aromatic amide	0.0076	3.3	434
44		Aromatic amide	0.0025	1.1	440

Inhibition constants ($K_{i(app.)}$) are given in μM.

Table 3. Enzyme inhibition data for compound **43**

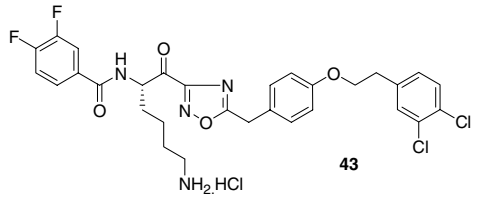

43

Potency (μM)	
Human B tryptase	0.0076
Mouse tryptase	0.365
Monkey tryptase	0.40
Selectivity (μM)	
Trypsin	3.3
Thrombin	>150
Plasmin	0.91
Kallikrein	83
APC	>150
Chymotrypsin	>150
Elastase	>150
Chymase	>150
Urokinase	>150
Granzyme K	>150
Cathepsin G	>150
Factor VIIa	>150
Factor Xa	>150
Factor IXa	>150
Factor XIa	>150

Table 4. Pharmacokinetic data for compound **44**

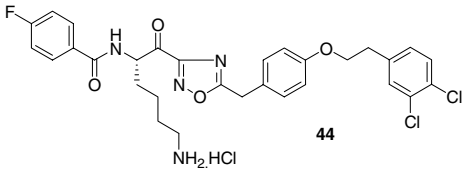

44

Potency (μM)	
Human B tryptase	0.0025
Mouse tryptase	0.365
Monkey tryptase	0.40
PK (0.5 mg/kg, iv, rat, $n = 3$)	
C_{max} (μM)	1.01 ± 0.25
CL (ml/min/kg)	45 ± 7.9
V_c (ml/kg)	457 ± 113
V_{ss} (ml/kg)	7800 ± 1280
MRT (min)	173 ± 14
AUC (μm min)	18 ± 3.3
Terminal half-life (min)	174 ± 16
PK (5 mg/kg, po, rat, $n = 3$)	
Absorption (%)	12
Bioavailability (%)	9
Terminal half-life (min)	135 ± 59

end we performed pharmacokinetic studies[18] on compound **44**, which showed a similarly high degree of selectivity against all proteases tested. Table 4 shows the results.

The long half-life values and mean residence time are consistent with limited first-pass metabolism. Thus, we achieved our intent of blocking metabolic hot-spots by use of the halogenated aromatic rings. The relatively low absorption (12%, cassette dosing) could be explained by a number of factors, including the relatively high molecular weight (599.5) of the parent free base of **44**, and also the presence of a primary amine function. That the oral bioavailability of 9% represented a high percentage (75%) of absorbed **44** suggested further evidence that first-pass metabolism pathways were curtailed.

In summary, we have demonstrated a series of highly potent and selective human tryptase inhibitors, an efficient method by which they can be prepared in library fashion, and finally, an example of a metabolically restricted compound member of the series that may be further developed as a possible therapy for indications implicated by excess mast-cell tryptase release.

References and notes

1. Cairns, J. A. *Pulm. Pharmacol. Ther.* **2005**, *18*, 55.
2. Payne, V.; Kam, P. C. A. *Anaesthesia* **2004**, *59*, 695.
3. Fiorucci, L.; Ascoli, F. *Cell. Mol. Life Sci.* **2004**, *61*, 1278.
4. Caughey, G. H. *Handbook of Proteolytic Enzymes*, 2nd ed., 2004; Vol. 2, p 1535.
5. Bradding, P. *Curr. Opin. Allergy Clin. Immunol.* **2003**, *3*, 45.
6. Newhouse, B. J. *IDrugs* **2002**, *5*, 682.
7. Abraham, W. M. *Am. J. Physiol.* **2002**, *282*, L193.
8. Gangloff, A. R. *Curr. Opin. Investig. Drugs (PharmaPress Ltd.)* **2000**, *1*, 79.
9. Rice, K. D.; Sprengeler, P. A. *Curr. Opin. Drug Discov. Devel.* **1999**, *2*, 463.
10. Rice, K.; Spencer, J. *Expert Opin. Ther. Patents* **1999**, *9*, 1537.
11. Elrod, K. C.; Numerof, R. P. *Emerging Therapeutic Targets* **1999**, *3*, 203.
12. Rice, K. D.; Tanaka, R. D.; Katz, B. A.; Numerof, R. P.; Moore, W. R. *Curr. Pharm. Des.* **1998**, *4*, 381.
13. Clark, J. M.; Moore, W. R.; Tanaka, R. D. *Drugs Future* **1996**, *21*, 811.

14. Rice, K. D.; Moore, W. R. *High Throughput Screen.* **2000**, 101.
15. Pereira, P. J. B.; Bergner, A.; Macedo-Ribeiro, S.; Huber, R.; Matschiner, G.; Fritz, H.; Sommerhoff, C. P.; Bode, W. *Nature (London)* **1998**, *392*, 306.
16. Sperandio, D. et al. *Bioorg. Med. Chem. Lett.* submitted for publication.
17. General inhibition assays—the active site concentrations of the various enzymes used for inhibition studies were determined through active site titration with 4-methylumbelliferyl *p*-guanidinobenzoate or were estimated from protein concentration measurements. Inhibitor potency measurements were performed at room temperature using a Molecular Device's SpectraMax 250 96-well kinetic plate readers. Reaction velocities were monitored at varying inhibitor concentrations by following the hydrolysis the liberation of *p*-nitroaniline (A_{405nm}). All substrates were added at concentrations equal to or near their K_m. All reactions were performed in a total volume of 100 μLs. Typically, enzyme and inhibitor were incubated 30 min prior to initiation of reaction with the addition of substrate. Control reactions in the absence of inhibitor were performed in parallel. The velocity of the enzyme-catalyzed reaction was determined from the linear portion of the progress curve, typically the first 5 min of the reaction after initiation with the addition of substrate. The K_i values were determined by a non-linear least squares regression fit of the experimentally derived data to the Morrison equation for tight-binding inhibitors as described (Kuzmic, P., et al., *Anal. Biochem.*, **2000**, *281*, p. 62). Example conditions for the tryptase and trypsin assays are provided below, other enzyme assays for which selectivity data are provided were performed in a similar manner. Example enzyme assay conditions Tryptase—tryptase (recombinant human Beta-1 from Promega) was incubated at 2 nM with variable concentrations of inhibitor in 50 mM Tris (pH 7.4), 150 mM NaCl, 0.02% Tween 20, 1 mM EDTA, 50 μg/ml heparin, and 10% DMSO. The reaction was initiated with substrate, Tosyl-Gly-Pro-Lys-pNA (Centerchem), supplied at the K_m (400 μM). The change in absorbance as a function of time was monitored at 405 nm.Trypsin—trypsin (Athens Research Institute) was incubated at 10 nM with variable concentrations of inhibitor in 50 mM Tris (pH 7.4), 150 mM NaCl, 1.5 mM EDTA, 0.05% Tween 20, and 10% DMSO. The reaction was initiated with substrate, Tosyl-Gly-Pro-Lys-pNA (Centerchem), supplied at the K_m (25 μM). The change in absorbance as a function of time was monitored at 405 nm.
18. Plasma concentrations of the compounds were determined by LC/MS/MS. The plasma sample was processed using acetonitrile precipitation, then the supernatant was injected onto the LC column. The limit of quantitation of the assay was 1–6 nM. Pharmacokinetic data were analyzed by WinNonlin-Pro (Pharsight Corp.), using compartmental and non-compartmental analysis for iv and po data, respectively. Pharmacokinetic parameters, including the area-under-the-curve (AUC), clearance (CL), volume of distribution (V_d), and mean residence time (MRT), were determined. Clearance and mean residence time were calculated as follows: CL = dose/AUC and MRT = V_d/CL. Oral absorption (Abs) and bioavailability (F) in rats were evaluated in portal vein (pv) and jugular vein (jv) cannulated animals. The plasma concentrations of the compounds in the portal and jugular vein were quantified and used to calculate the area-under-the-curve (AUC). Oral absorption and bioavailability were calculated from dose-normalized AUC values as follows: $Abs = AUC_{po,pv}/AUC_{iv,jv}$ and $F = AUC_{po,jv}/AUC_{iv,jv}$.